Volume 12 Number 4 1984 Nucleic Acids Research

Physical properties of the *E. coli* 4.5S RNA: first results suggest a hairpin helix of unusual thermal stability

David B.Bourgaize, Cathy Farrell, Kenneth H.Langley+ and Maurille J.Fournier

Departments of Biochemistry and +Physics, University of Massachusetts, Amherst, MA 01003, USA

Received 26 September 1983; Revised and Accepted 20 January 1984

ABSTRACT

Hyperchromicity measurements and quasi-elastic laser light scattering (QELS) have been used to assess the solution structure of the metabolically stable E. coli 4.5S RNA Results from thermal denaturation measurements revealed the 4.5S species to be markedly more stable than most other RNAs characterized thus far. Optical Tm's range from 79° to 88° with transitions ~25°C wide The Tm values show little dependence on ionic strength, but stability is enhanced considerably by Mg^{+2}. In the QELS experiments the diffusion coefficient does not decrease until T > 70°C. Neither the diffusive melting nor the diffusion coefficient at infinite dilution ($D^{\circ}_{20,w}$) show dependencies on ionic strength but both are influenced by Mg^{+2}. The diffusion behavior is in agreement with that predicted for a rigid cylindrical molecule 125 to 160 Å long and 37 to 26 Å in diameter. Taken together these results are consistent with the more stable hypothetical secondary structures that can be formed, in which 70-75% of the 114 bases are paired to form a single extended hairpin helix.

INTRODUCTION

The E. coli 4.5S RNA is a small, metabolically stable species that normally occurs in the cell at the level of a single tRNA. Although it was one of the first RNAs to be sequenced (1) it has received only slight attention since and its function is not yet known. Biosynthesis of this species has been shown to be under stringent control (2) and to involve nucleolytic processing by RNAse P, a tRNA maturation enzyme (3). Together these latter findings suggest that this species may have a tRNA-related function. Inspection of the nucleotide sequence suggested that the 4.5S RNA may be structurally unique compared with other small RNAs such as tRNA and 5S RNA. In this regard it was possible to fold the sequence into a highly paired, extended stem-loop structure (1).

Our laboratory has recently initiated work on the 4.5S RNA and its gene with a view to characterizing its synthesis, structure and function. To this end the gene has been cloned and sequenced and shown by genetic means to be required for cell viability. Recombinant strains which overproduce the

4.5S RNA by 15-30 fold have also been developed, making it more feasible to undertake detailed studies of the RNA itself. In the condition of greatest abundance the 4.5S species corresponds to about 65% of the total small RNA, making it some 4-5 times more abundant than the 5S ribosomal RNA. These various results will be presented elsewhere (Hsu et al., Brown and Fournier, Bourgaize et al., in preparation).

The RNA sequence deduced from the DNA sequence is longer and slightly different from that developed in the original RNA fingerprinting analysis. The new sequence, shown in Figure 1, consists of 114 bases which can be folded into a near-perfect hairpin structure. The G + C content is 64%. In the particular hypothetical structure shown 86 of the bases are involved in secondary base pairs, corresponding to 75% of the total nucleotides. In the case of tRNAs and the small ribosomal RNAs the degree of secondary pairing is considerably lower at 45-50%.

Structural analysis of the 4.5S RNA is desirable from two perspectives. One of course, relates to the eventual identification of important structure-function relationships. The second is the attraction of characterizing a new RNA form with potentially unique structure. In this regard most of our detailed knowledge of RNA structure has come from analyses of tRNA. This situation is due to their relatively small size and greater natural abundance. The availability of our over-producing 4.5S RNA gene clones provides the opportunity to initiate in-depth structure studies of a unique new class of small RNA.

In this paper we present results from two physical studies of the 4.5S RNA. These analyses, the first to be carried out on the molecule, include evaluation by absorbance hyperchromicity and quasi-elastic laser light scattering (QELS). The hyperchromicity method is useful in assessing base-base interactions and overall thermal stability in different solution conditions. With the QELS technique information about translational diffusion behavior provides additional insight into stability, shape and effects of solution conditions on hydrodynamic behavior. Measurements of the translational diffusion coefficient can also give valuable information about tertiary-level conformational changes. Of special interest in this first analysis was an examination of thermal stability and diffusion behavior with a view to assessing hypothetical secondary structures that can be generated from the primary structure. The results show clearly that the 4.5S RNA does indeed possess an unusually high degree of secondary structure and that a folding scheme such as that shown in Figure 1 is consistent with the behavior observed.

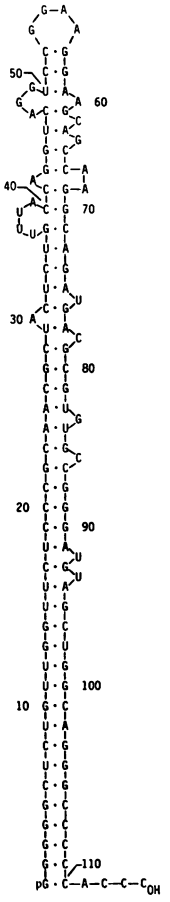

Figure 1: Sequence and hypothetical secondary structure of the E. coli 4.5S RNA. The primary structure was deduced from the DNA sequence of the cloned gene (Hsu et al., in preparation). The hydrogen-bonding scheme shown for the secondary structure was derived by maximizing the free-energy of folding using the pairing rules of Tinoco et al. (4). In this arrangement the molecule has 43 base pairs, involving 75% of the 114 nucleotides and has a calculated ΔG of -60 kcal/mole. The GC-content is 64%.

METHODS

Preparation of 4.5S RNA--All 4.5S RNA was isolated from E. coli JA221 (lacY, leuB6, trpE5, hsdM$^+$, hsdR$^-$, recA-1, C600 background) harboring plasmid pLH45-1, a pBR322 derivative with the 4.5S DNA cloned into the tetracycline-resistance gene. ^{32}P-RNA was prepared by in vivo labeling in MOPS/glucose medium containing 20 μg/ml ampicillin (5); MOPS is morpholinopropane sulfonate. 0.5 ml of overnight culture was used to inoculate 2 flasks containing 50 ml of the same medium. 15 mCi ^{32}P-orthophosphate (New England Nuclear) was added to one flask while the second served as a reference culture. Cells were grown at 37°C until the optical density was A_{600} = 1.0 and then harvested by centrifugation. Total small RNA was prepared by phenol extraction as described elsewhere (6). The RNA was fractionated electrophoretically in a 40 cm x 17 cm x 2 mm 10% polyacrylamide gel under

the conditions cited below. The desired bands were located by autoradiography, excised and the 4.5S RNA eluted by soaking in an elution buffer containing 0.5 M ammonium acetate, 10 mM magnesium acetate, 1 mM EDTA, 0.1% sodium dodecyl sulfate. After ethanol precipitation, the purity and integrity of the molecule was assessed by acrylamide gel electrophoresis.

Unlabeled 4.5S RNA was purified by chromatography on benzoylated diethylaminoethyl-cellulose (BD-cellulose; Boehringer Mannheim) and Sepharose 4B (Pharmacia) followed by preparative acrylamide gel electrophoresis. E. coli JA221/pLH 45-1 was grown in L-broth medium until A_{600} = 1.0. Small RNA was prepared by phenol extraction and ethanol precipitation as above. The precipitate was solubilized in 50 mM Tris·HCl, pH 7.5, 0.1 M NaCl, 10 mM $MgCl_2$. After precipitation with ethanol, the sample was solubilized in 10 mM sodium acetate, pH 4.5, 0.4 M NaCl, 10 mM $MgCl_2$. 800,000 cpm ^{32}P-4.5S RNA was added as a tracer and the mixture applied to a 1.5 m x 1.5 cm BD-cellulose column previously equilibrated with the same buffer. The RNA was eluted in 5 ml fractions with a 4-L linear sodium chloride gradient with limits of 0.4 M and 1.0 M. The fractions containing 4.5S RNA were pooled, precipitated, resolubilized and applied to a 60 cm x 2.5 cm Sepharose 4B column equilibrated with 10 mM sodium acetate, pH 4.5, 1.3 M ammonium sulfate, 6 mM 2-mercaptoethanol, 10 mM $MgCl_2$, 1 mM EDTA. RNA was eluted in 5 ml fractions with a 3-L reverse gradient with limits of 1.3 M and zero ammonium sulfate (7). The 4.5S RNA fractions were pooled and precipitated and the RNA further enriched by electrophoresis in a 40 cm x 17 cm x 3 mm 10% polyacrylamide gel; electrophoresis was for 20 hrs at 4 mA. The desired bands were located by UV shadowing, excised, and the RNA recovered by extraction in the gel elution buffer described above. The recovered material was passed over a 1 ml DEAE-cellulose column to remove residual acrylamide using conditions described above. The purity of the resulting 4.5S RNA was analyzed on 10% polyacrylamide gels under both denaturing and non-denaturing conditions. Owing to its unusual stability an acid-urea system (sodium citrate, pH 3.5, 6 M urea) was used to achieve complete denaturation (8).

Sample Preparation for Hyperchromicity Experiments--All measurements were made in 10 mM sodium cacodylate, pH 6.8, with $MgCl_2$ concentration and total ionic strength-adjusted with NaCl, as variables. The RNA samples, typically 15-20 µg/ml, were dialyzed against the test solution prior to analysis. To create the zero magnesium condition, the sample was heated to 85°C for 10 minutes in solution containing 2 mM Hepes, pH 7.0, 0.5 M NaCl, 10 mM EDTA, dialyzed against the same buffer, then against the solution

condition to be evaluated. Samples were degassed under vacuum prior to measurement.

Sample Preparation for QELS--Thirty µl samples at concentrations typically 8-10 mg/ml were dialyzed against the appropriate test solution. Samples were preheated for 5 minutes at 37°C, then filtered (Hamilton Syringe, Millipore 0.22 µM filter), half into an equal volume of filtered buffer, half directly into a 2 mm x 2 mm quartz cuvette (Precision Cells) in which the measurements were made. In this manner, 4-6 serial dilutions were prepared for each solution condition evaluated. After measurement, the sample was diluted and the RNA concentration determined spectrophotometrically.

Hyperchromicity Measurements--Measurements were performed with a Beckman Model 35 double-beam spectrophotometer with a jacketed cell holder and 1 cm quartz cuvettes. A copper-constantan thermocouple junction was inserted directly into the solution through a teflon cap. A Haake FE programmable circulating water bath was used to heat the sample from 25°-100°C linearly at a rate of 2°C per minute. In each case the melt was repeated using the same sample to insure reproducibility. Evaporation was accounted for by using a control solution of CTP. Since the nucleotide was free in solution, any observed increase in absorbance was presumed to be due to evaporation. The amount of evaporation was corrected for in subsequent measurements. After measurement, sample integrity was evaluated by denaturing acrylamide gel electrophoresis. In each case the experimental material was found to co-migrate with intact, untreated 4.5S RNA.

QELS Measurement--Measurements were performed as described previously (9). To assess possible evaporation effects during thermal denaturation experiments, the diffusion coefficient of 0.085 µM diameter polystyrene beads (Dow Chemical) was monitored throughout the temperature range used and found to remain constant. Extrapolation of averaged $D_{20,w}$ data to zero RNA concentration gives $D^{\circ}_{20,w}$. Error within a data set is typically ~1%.

RESULTS

4.5S RNA Purification--4.5S RNA was purified by successive enrichment on columns of BD-cellulose and Sepharose 4B followed by electrophoresis in polyacrylamide. ^{32}P-4.5S RNA was added to the crude RNA to permit rapid identification of fractions containing the 4.5S species. Figure 2 shows the fractionation pattern obtained with BD-cellulose. Fractions with 4.5S RNA (#69-131) were pooled, ethanol precipitated, and the RNA further enriched by

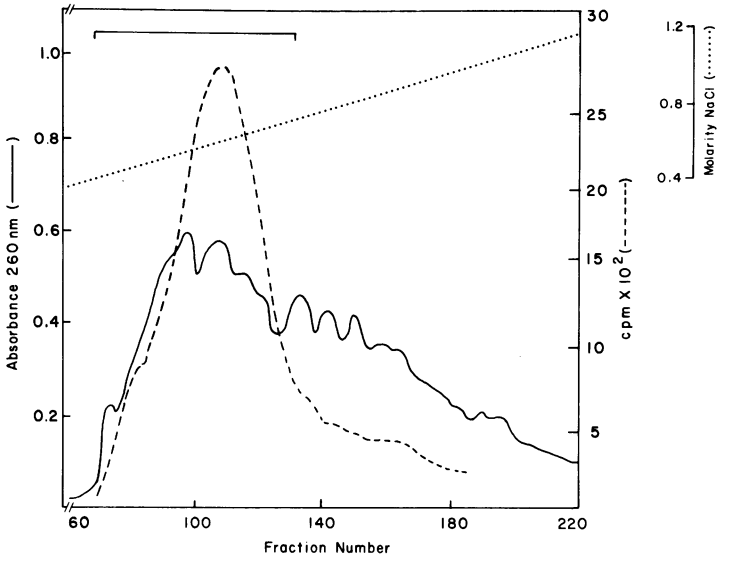

Figure 2: Fractionation of E. coli small RNA by BD-cellulose chromatography. 1.4 g RNA with 8 x 10^5 cpm ^{32}P-4.5S RNA as tracer was loaded onto a 1.5 m x 2.5 cm column equilibrated in 10 mM sodium acetate, pH 4.5, 0.4 M NaCl, 10 mM $MgCl_2$. The column was developed with a 4L linear gradient from 0.4 to 1.0 M NaCl at a flow rate of 1 ml/min. (——) absorbance at 260 nm; (---) ^{32}P-cpm; (···) NaCl conc.

reverse ammonium sulfate gradient fractionation on Sepharose 4B. The elution profile obtained, Figure 3, shows three principle peaks. Electrophoretic analysis of the material in pooled fractions 215-220 showed the RNA to consist solely of 4.5S and 5S RNA in a ratio of approximately 5:1. The material in fractions 150-185 proved to be mostly tRNA and that in fractions 115-150 to be higher molecular weight aggregates of 4.5S RNA. Final purification of the 4.5S RNA was by preparative gel electrophoresis in 10% polyacrylamide. Figure 4 shows the resulting material to be at least 90% pure by electrophoresis in both denaturing and non-denaturing conditions (see Methods).

Hyperchromicity Experiments--The change in absorbance at 260 nm was observed as a function of temperature as described in the Methods section. The Tm value is taken as the temperature at the midpoint of the transition, and is used as a measure of the stability of the molecule. In Figure 5 are shown typical melting curves obtained for the 4.5S RNA in zero, 1 and 5 mM

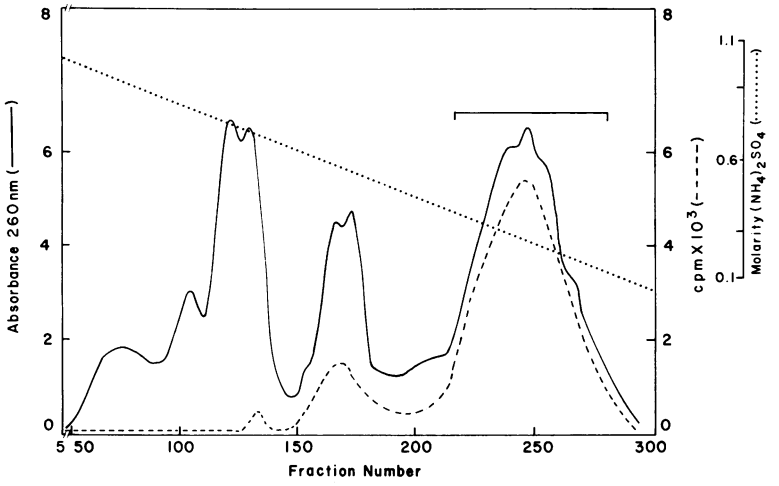

Figure 3: Enrichment of 4.5S RNA by reverse salt gradient elution from Sepharose 4B. 500 mg BD-cellulose enriched RNA was applied to a 60 cm x 2.5 cm column of Sepharose 4B previously equilibrated with high salt buffer as described in Methods. The RNA was eluted with a 3L reverse ammonium sulfate gradient, from 1.3 M to zero $(NH_4)_2SO_4$, at a flow rate of 1 ml/min. (——) absorbance at 260 nm; (---) cpm; (···) molarity of ammonium sulfate.

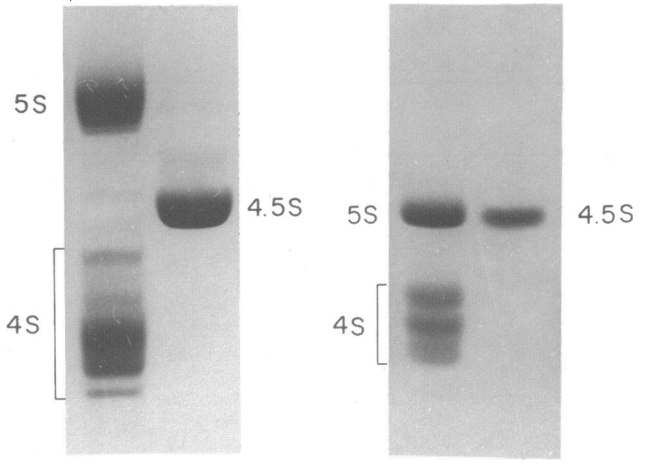

Figure 4: Gel electrophoresis of enriched 4.5S RNA. 4.5S RNA samples were analyzed electrophoretically on gels of polyacrylamide, (1 mm thickness) as described in Methods. Standards are a mix of bulk E. coli tRNA enriched by Sephadex G-100 gel filtration chromatography, and E. coli 5S RNA purified by RPC-5 reverse phase chromatography. Left panel, native condition, 6 µg 4.5S RNA; right panel, acid-urea denaturing condition, 3 µg 4.5S RNA.

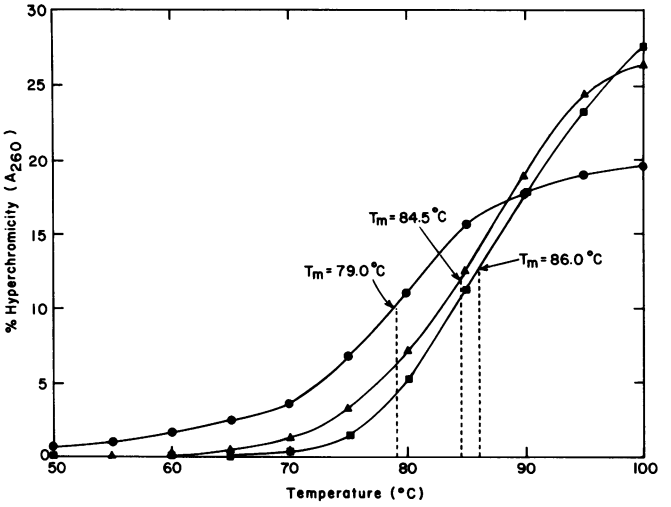

Figure 5: Thermal denaturation of 4.5S RNA. Measurements of A_{260} as temperature was increased were performed as described in Methods. The midpoint of the transition is the T_m. Samples were in 10 mM sodium cacodylate, pH 6.8 with variable Mg^{+2} concentration but constant ionic strength of 0.1 M; (-●-) zero Mg^{+2}; (-▲-) 1 mM Mg^{+2}; (-■-) 5 mM Mg^{+2}.

TABLE I

Thermal Denaturation Properties of E. coli 4.5S RNA

μ(M)	Mg^{+2}(mM)	Tm(°C ± 0.5)	% Hyperchromicity (± 1)	Transition Width (°C ± 2)
0.05	1	85.5	22	26
0.05	10	86.5	24	23
0.10	0	79.0	20	27
0.10	1	84.5	24	23
0.10	2	86.2	22	22
0.10	5	86.0	26	27
0.10	10	88.5	19	19
0.25	0	82.5	25	25
0.25	1	84.5	27	25
0.25	2	83.0	29	27
0.25	5	85.5	25	24
0.25	10	85.5	25	19

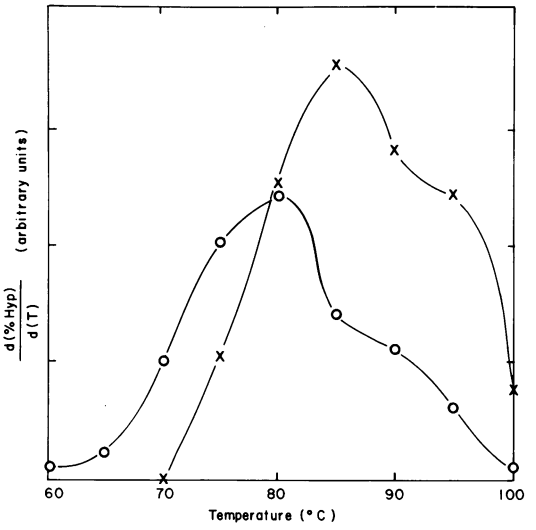

Figure 6: Differential plot of 4.5S RNA hyperchromicity vs temperature. The change in hyperchromicity with temperature is shown for two conditions of magnesium at μ = 0.1 M. (-o-) zero Mg^{+2}; (-x-) 5 mM Mg^{+2}.

Mg^{+2} at an ionic strength of 0.1 M. Here, Tm values from 79° to 86°C were observed, with greatest stability evident when magnesium was present.

Results for a variety of solution conditions where Mg^{+2} and ionic strength were varied are shown in Table 1. In all conditions evaluated, the observed melting temperatures are high for a small RNA species, indicative of unusual stability In some cases, denaturation was still incomplete at 100°C (Figure 5, 5 mM Mg^{+2} data). Denaturation was observed to be more cooperative with magnesium present, as judged by the width of the transition. As indicated in Table I the melting temperature is relatively insensitive to changes in ionic strength, except where magnesium is absent. In this case, higher ionic strength stabilizes the molecule. However, magnesium has a more pronounced effect upon stability. At lower ionic strengths (μ = 0.1 M), the Tm changes from 79°C at 0 mM Mg^{+2} to 88°C at 10 mM Mg^{+2}. At higher ionic strength (μ = 0.25 M), magnesium still increases stability, but to a lesser degree.

A differential plot of hyperchromicity versus temperature reveals that denaturation is not fully cooperative. As seen in Figure 6, regions of differing thermal stability exist. The major peak coincides with the Tm, while at least one other transition is evident ~10 degrees higher. While this is a very low resolution method of analysis, it does provide evidence

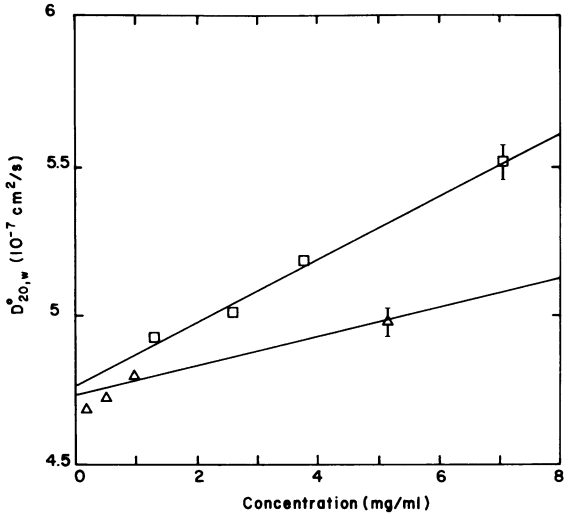

Figure 7: RNA concentration dependence of the translational diffusion coefficient of 4.5S RNA. $D_{20,w}$ was measured as described in Methods for solutions that were 10 mM sodium cacodylate, pH 6.8, 10 mM Mg^{+2} and either 0.1 M or 0.25 M ionic strength, the latter adjusted with NaCl. Extrapolation to zero RNA concentration gives $D^{\circ}_{20,w}$. Error bars indicate the largest error within a data set. (-□-) μ = 0.1M; (-△-) μ = 0.25 M.

for at least two regions of differing stability.

QELS Experiments--The measured translational diffusion coefficient, D, is corrected to 20°C in water ($D_{20,w}$). When plotted versus RNA concentration, the value of $D_{20,w}$ extrapolated to zero RNA gives $D^{\circ}_{20,w}$. Typical plots of translational diffusion coefficient versus RNA concentration are shown in Figure 7. The differences in slope seen for the two conditions can be shown to be due to the ionic strength difference between samples.

There is a dependence of $D^{\circ}_{20,w}$ upon magnesium concentration at a given ionic strength (see Fig. 8). At 2 mM Mg^{+2}, the diffusion coefficient is highest for all ionic strengths tested with a subsequent 5-10% decrease as magnesium is increased to 5 mM. Further increases in Mg^{+2} raise the diffusion coefficient value only slightly.

At Mg^{+2} concentrations of 2 mM and above, changes in ionic strength do not greatly effect the diffusion coefficient (Fig. 8). At 1 mM Mg^{+2}, however, increasing ionic strength brings $D^{\circ}_{20,w}$ closer to the values observed at 2 mM Mg^{+2}. This suggests that at lower Mg^{+2}, salt can mimic the effect of magnesium ion, while at higher Mg^{+2} levels a specific effect of magnesium may be present.

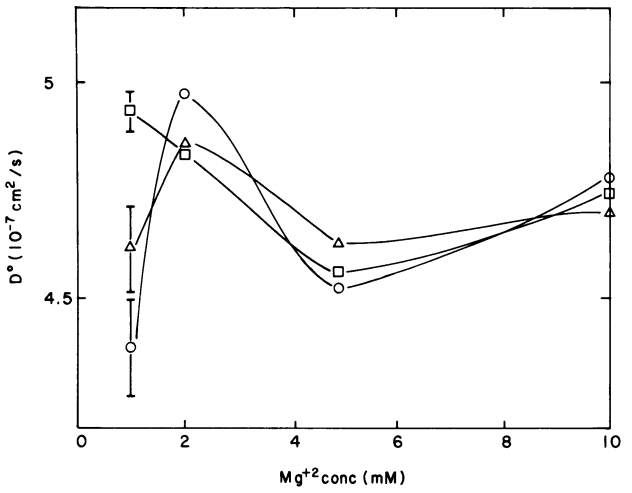

Figure 8: Effects of magnesium on the diffusion behavior of 4.5S RNA. $D^\circ_{20,w}$ values were determined as described in Figure 7 and Methods for RNA in solution containing 1 to 10 mM Mg^{+2} at constant ionic strength. The ionic strengths evaluated ranged from 0.10 to 0.25 M. The values for μ were: (-o-) 0.1 M; (-Δ-) 0.15 M; (-□-) 0.25 M. The error within a data set is ∿1% except for two of the three 1 mM Mg^{+2} conditions.

Thermal denaturation of the 4.5S RNA was also followed hydrodynamically by measuring $D_{20,w}$ as a function of temperature. The relative change in translational diffusion coefficient with temperature is shown for typical solution conditions in Figure 9. Generally, an increase in relative diffusion coefficient of 6-10% is seen as the temperature goes from 50°C to 70-80°C. After reaching a peak slightly below the optical Tm, the relative diffusion coefficient decreases sharply as temperature is further increased. The effect of increased magnesium, as seen in Figure 9, is to shift the melting profile to higher temperatures; no dependence on ionic strength is observed. This result is similar to that observed in the hyperchromicity experiments, showing that magnesium stabilizes the molecule.

The increase in relative diffusion coefficient seen prior to melting is an interesting feature. It suggests that an alternate stable conformation may exist at higher temperatures, different from that at 20°C.

Hydrodynamic Model

The value of the measured diffusion coefficient clearly shows that the molecule must be in a highly base paired, extended conformation. A calculation of D for a compact spherical shape of reasonable molecular volume, for

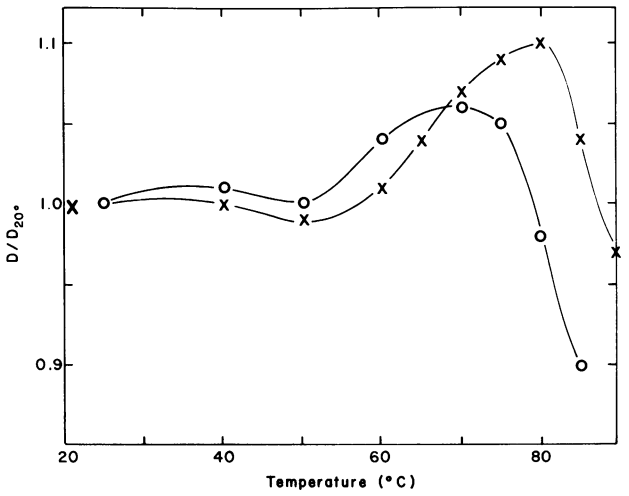

Figure 9: Laser light scattering analysis of 4.5S RNA thermal denaturation. Relative change in translational diffusivity is shown as a function of temperature. $D_{20,w}$ values were determined as described in Methods and Figures 7 and 8 for RNA in solutions of 0.1 M ionic strength and 1 or 10 mM Mg^{+2}. The relative diffusion values were corrected to 20°C. (-o-) 1 mM Mg^{+2}; (-x-) 10 mM Mg^{+2}.

example, yields $D^{\circ}_{20,w} \approx 8 \times 10^{-7}$ cm^2/sec, which is much too large to be consistent with the data. We therefore choose a more plausible shape, that of a cylinder.

Using the theory of Broersma (10), the diffusion coefficient of a rigid cylindrical molecule can be calculated given its length and diameter:

$$D = \frac{kT}{3\pi\eta_o L}\left(\delta - \frac{1}{2}\left[1.27 - 7.4\left(\frac{1}{\delta} - 0.34\right)^2\right] - \frac{1}{2}\left[0.19 - 4.2\left(\frac{1}{\delta} - 0.39\right)^2\right]\right)$$

where

D = translational diffusion coefficient (cm^2/sec)

k = Boltzman's constant

T = temperature (°K)

η_o = solution viscosity (poise)

L = length (cm)

d = diameter (cm)

$\delta = \ln(\frac{2L}{d})$

Values for the length and diameter obtained from the model shown in Figure 1 are 160 Å and 26 Å, respectively. These estimates are based on a

molecular length of 43 base pairs x 2.5 Å per stacked base, plus an additional 30 Å due to unpaired helix bases and 20 Å from the 3'-tail and hairpin loop; a helix diameter of 26 Å is assumed. These final dimensions ignore the bulges and loops in the helical structure, but do assume a hydration layer of 3-4 Å around the molecule. Using these values, a diffusion coefficient of 4.8 x 10^{-7} cm^2/sec is obtained, close to the average $D^{\circ}_{20,w}$ observed experimentally.

The same diffusion coefficient can be derived from the rigid cylindrical model by assuming a decreased length and correspondingly increased effective diameter up to a limit of about L = 125 Å and d = 37 Å. For any length less than this, the calculated D is much larger than that observed, independent of the assumed diameter. Since it is difficult to imagine a helix diameter of less than 26 Å (including hydration layer), the length is rather firmly bounded in the range of 125 to 160 Å with a corresponding average diameter of 37 to 26 Å which would include any effects of small side loops, bends, zigzags, or lack of base pairing in the apex region. Thus, the hydrodynamic measurements are completely consistent with a highly base paired structure in which the 4.5S RNA molecule is seen as an extended helical hairpin. The low diffusion coefficient observed argues against a high degree of molecular flexibility, since flexibility would increase that value.

In theory, a frictional ratio can be obtained from the measured diffusion coefficient. However, due to uncertainties in values for the partial specific volume of the molecule, these calculations were not performed.

DISCUSSION

The melting temperatures observed in these experiments are unusually high compared to those for other small RNA species and exhibit greater cooperativity. Table II compares hyperchromicity properties for various small RNA molecules and DNA. The data for the 4.5S RNA show that this molecule exhibits stability and cooperativity more comparable to DNA than to most small RNA species. In a solution condition of 0.1 M ionic strength and zero Mg^{+2}, the melting temperature is 79°C and the transition is 27°C wide. Under similar conditions tRNAs and 5S RNA have Tm values in the range of 50-60°C and transitions of ∿40°. This high thermal stability is strong evidence for a molecule with an extensive degree of secondary structure.

The results from the QELS experiments confirm this conclusion; thermal denaturation is not observed until the temperature reaches 70-80°C. In

TABLE II

Thermal Denaturation Properties of Assorted Nucleic Acids

Nucleic Acid	Tm(°C)	Width(°C)	Reference
Yeast $tRNA_1^{Ala}$	60†	40	(11)
Yeast $tRNA^{Phe}$	50	40	(12)
E. coli 5S RNA	59	40	(13)
Calf thymus DNA	87	15	(14)
E. coli 4.5S RNA	79	27	This Study

†major transition

addition both experimental methods give evidence of regions of differing stability within the molecule, if not entirely different conformations. The presence of at least two distinct melting domains is indicated by the differential plot of hyperchromicity vs temperature. Here, a second transition occurs ∿10°C above the main transition which corresponds to the Tm. The QELS results give an indication of the existence of an alternative conformation at temperatures below those at which thermal denaturation is achieved. This form is characterized by a 6-10% higher diffusion coefficient than at lower temperatures. In the model of Figure 1 the region of the structure from base 36 to 71 can be predicted to be less stable than the rest of the molecule. It is conceivable that this region could undergo a rearrangement that results in a more compact hydrodynamic structure.

It is well established that mono- and divalent cations can interact with polyelectrolytes such as RNA in various ways. Generally, higher ionic strengths will stabilize nucleic acids resulting in increased melting temperatures (15). As expected this was also observed for the 4.5S RNA. The effect is most notable in the absence of magnesium, in which case increasing ionic strength from 0.1 to 0.25 M increases the melting temperature from 79 to 82°C. In addition, at 1 mM Mg^{+2}, the translational diffusion coefficient increases ∿10% as the ionic strength is raised from 0.1 to 0.25 M. When magnesium is present in higher concentrations, the effect of increasing salt becomes negligible. These results suggest that mono- and divalent cations play a similar role in stabilization, but that there may be additional unique effects of magnesium at higher concentrations. Perhaps there are unique binding sites for magnesium on the 4.5S RNA molecule, as has been reported

for tRNA (16-18).

Considered together, the physical evidence presented here argues strongly for an extended, helical structure for the 4.5S RNA molecule. The high melting temperatures observed by both methods indicate a high degree of base pairing. The cooperativity of the optical melts reflects a high degree of helical structure and the results from the hydrodynamic measurements suggest that a somewhat rigid, extended conformation is adopted by this molecule in solution. The Broersma theory for rigid cylindrical molecules gives a molecular size and shape estimate that is in good agreement with the postulated secondary structure presented here. These results are all consistent with the model presented, that of a highly base-paired, helical hairpin structure. Higher resolution analyses are now in progress to more accurately define the structure of this unique molecule and genetic and biochemical strategies are in use to identify its biological function.

ACKNOWLEDGEMENT

The assistance of Manuel Tsiang with the early hyperchromicity analyses is gratefully acknowledged. This work was supported by a NIH grant to MJF (GM 19351) and a NSF grant to KHL (PCM 80-21136).

REFERENCES

1. Griffen, B. E. (1975) J. Biol. Chem. 250, 5426-5437.
2. Bothwell, A. L. M., Garber, R. L. and Altman, S. (1976) J. Biol. Chem. 251, 7709-7716.
3. Ikemura, T. and Dahlberg, J. E. (1973) J. Biol. Chem. 248, 5033-5041.
4. Tinoco, Jr., I., Borer, P. N., Dengler, B., Levine, M. D., Uhlenbeck, O. C., Crothers, D. M. and Gralla, J. (1973) Nature 246, 40-41.
5. Neidhart, F. C., Bloch, P. L. and Smith, D. F. (1974) J. Bacteriol. 119, 736-747.
6. Fournier, M. J. and Peterkofsky, A. (1975) J. Bacteriol. 122, 539-548.
7. Holmes, W. M., Hurd, R. E., Reid, B. R., Rimerman, R. A. and Hatfield, G. W. (1975) Proc. Natl. Acad. Sci. U.S.A. 72, 1068-1071.
8. Pedersen, F. S. and Haseltine, W. A. (1980) Methods Enzymol. 65, 680-687.
9. Olson, T., Fournier, M. J., Langley, K. H. and Ford, Jr., N. C. (1976) J. Mol. Biol. 102, 193-203.
10. Broersma, S. (1960) J. Chem. Phys. 32, 1632-1635.
11. Riesner, D., Romer, R. and Maass, G. (1969) Biochem. Biophys. Res. Commun. 35, 369-376.
12. Romer, R., Riesner, D., Maass, G., Wintermeyer, W., Thiebe, R. and Zachau, H. G. (1969) FEBS Lett. 5, 15-21.
13. Marsh, T. (1981) Ph.D. Thesis, University of Massachusetts.
14. Doty, P. (1962) in "The Structure and Biosynthesis of Macromolecules", Biochemical Society Symposia, No. 21, Cambridge University Press, New York.
15. Marmur, J. and Doty, P. (1962) J. Mol. Biol. 5, 109-118.

16. Kallenbach, N. R. and Berman, H. M. (1977) Quarterly Rev. Biophys. 10, 138-236.
17. Maruyama, S. and Sugai, S. (1980) J. Biochem. 88, 151-158.
18. Schimmel, P. R. and Redfield, A. G. (1980) Ann. Rev. Biophys. Bioeng. 9, 181-221.